Diols as Solvent Media for Liquefaction of Corn Stalk at Ambient Pressure

Yan Zhang, Zhong Liu,* Lanfeng Hui,* and Huimei Wang

The proper selection of solvents is important during liquefaction of biomass process to produce fuel additives and valuable chemicals. In this study, novel low-cost liquefying agents such 1,2-propanediol (PG), diethylene glycol (DEG), and 1,4-butanediol (BDO), as well as the traditional liquefying agent, ethylene glycol (EG), were used. It was found that the liquefaction yield of corn stalk in the presence of PG at the optimum temperature of 180 °C was up to 99.2%, which was higher than that of the other three liquefying agents. The main components and functional groups of bio-oil with an acid catalyst were characterized by gas chromatography-mass spectrometry (GC-MS) and Fourier transform infrared spectroscopy (FTIR). The chief constituents of bio-oil were complex, and corn stalk could be effectively degraded with PG liquefaction. Moreover, the thermogravimetric analysis (TGA), X-ray diffraction (XRD), and scanning electron microscopy (SEM) data also revealed that the fiber structure of the liquefied corn stalk was destroyed and essentially liquefied during PG liquefaction. Consequently, all the results in the study successfully confirmed that PG can provide an efficient and environmental process for generating bio-oil from lignocellulosic mass at a low cost in liquefaction of corn stalk.

Keywords: EG; DEG; BDO; PG; Liquefying agent

*Contact information: Tianjin Key Lab of Pulp & Paper, Tianjin University of Science & Technology, Tianjin 300457, China; *Co-Corresponding author, E-mail: mglz@tust.edu.cn; huipeak@163.com*

INTRODUCTION

Given the exhaustion of fossil energy sources and environment deterioration, finding inexpensive, sustainable, and compatible petrochemical liquids to be used as transportation fuels is of tremendous interest (Saxena *et al.* 2009). Biomass sources include agroforestry, animal waste, industrial waste, waste water and waste residue, domestic waste, and aquatic life (Saidur *et al.* 2011). Owing to the large amount, low environmental effect, and reproducibility, plant biomass chemical technology has become one of the main sources of energy. High-value liquid and gas products that can be used as effective clean energy sources are of great importance (Field *et al.* 2008). Lignocellulosic resources from wood, corn stalk, bagasse, and other biomass resources are expected to be less expensive, more sustainable, and more environmentally friendly. Hence, further research and developing biomass resources is of historic strategic significance.

Biomass liquefaction is a technology that can effectively transform biomass resources, and it has attracted attention from researchers worldwide (Vasilakos and Austgen 1985; Pu and Shiraishi 1994; Xu and Etcheverry 2008; Lee *et al.* 2015a; Breunig *et al.* 2017). Converting biomass into liquid using the proper temperature, pressure, solvent, and catalyst is a thermochemical process (Minowa *et al.* 1997; Demirbaş 2001; Hatfield and Vermerris 2001; Minowa *et al.* 2004). Its products can substitute

petrochemical products and can be further processed as chemical raw materials for manufacturing other products.

Liquefaction can be divided into two categories. One category involves retaining the macromolecular structure of the plant fiber to prepare natural polymer materials. For example, fiber is used as raw material to produce polyurethane foams (Yao *et al.* 1995), phenolic resins (Kobayashi *et al.* 2001; Tymchyshyn and Xu 2010), carbon fibers (Yoshida *et al.* 2005), and adhesives (Kunaver *et al.* 2010). The second category involves the destruction of the large molecular structure of the raw materials to turn plant fiber into small molecules, such as ethanol (Nikolić *et al.* 2008) and biofuel oil (Stiller *et al.* 1996; Minowa *et al.* 1998).

The key difference between liquefaction and the other three thermochemical conversion processes (combustion, pyrolysis, and gasification) is that water or other suitable solvents must be adopted as the reaction medium during the liquefaction process (Yip *et al.* 2009). The phenol liquefaction of wood often uses a variety of catalysts to promote the reaction, including acid, alkali, and salt catalysts (Minowa *et al.* 1997; Alma *et al.* 1998). Pu and Shiraishi (1993a,b) used phenol to liquefy wood without a catalyst. The results showed that a 250 °C temperature and a time frame of a few hours were the optimal conditions for the reaction in which the products could be dissolved in a water and 1,4-dioxane mixed liquid.

Because the liquefaction involves the use of phenol, it has a certain degree of toxicity. Moreover, it was difficult to find the right balance of temperature, time, and pressure for this process. Therefore, many scholars began to study the use of polyols to liquefy lignocellulosic materials. Other researchers (Yao *et al.* 1994; Shiraishi *et al.* 1996; Yu *et al.* 2006b; Lee *et al.* 2015b) adopted alcohols such as ethylene glycol (EG), polyethylene glycol (PEG), and glycerin instead of phenols as liquefaction solvents and were able to liquefy lignocellulosic materials almost completely in the presence of acid catalysts at a certain temperature, under atmospheric pressure. Cyclic carbonates are also used as liquefaction agents because of their high dielectric constants, polarity, and reactivity. Lignocellulosic materials such as wood and cellulose have been liquefied using ethylene carbonate (EC) or propylene carbonate (PC) in the presence of an acid catalyst at elevated temperatures. The EC-liquefaction of cellulose and white birch were very rapid and complete processes (Yamada and Ono 1999). However, while lignocellulosic materials can be liquefied using cyclic carbonate, the reaction mechanism is unclear. Moreover, the associated costs are high.

The objective of this study was to select an effective and inexpensive polyol liquefying agent able to perform under relatively mild conditions. The degradation of cellulose, hemicellulose, and lignin from corn stalk and the influence of temperature on liquefaction were studied to evaluate the effect of the liquefying agent (1,2-propanediol (PG), 1,4-butanediol (BDO), and diethylene glycol (DEG)) on the liquefaction process after catalysis using concentrated phosphoric acid. The results were compared with those of the traditional liquefaction using EG. The liquefaction residue and bio oil obtained at the most suitable temperatures for each liquefaction agent were characterized by Fourier transform infrared spectroscopy (FTIR), gas chromatography-mass spectrometry (GC-MS), thermogravimetric analysis (TGA), X-ray diffraction (XRD), and scanning electron microscopy (SEM).

EXPERIMENTAL

Materials

Corn stalk (20- to 80-mesh) obtained from a farmland in Tianjin, China. It was dried in an oven at 105 °C for 12 h and stored in a desiccator before use. The chemical composition of the corn stalk was summarized in Table 1.

Table 1. Chemical Composition of Corn Stalk

Chemical Constituent	Extract	Cellulose	Hemicellulose	Lignin	Ash	Moisture
Mass fraction (%)	13.80	36.89	20.42	17.38	2.43	7.12

The main chemicals concentrated phosphoric acid, 1,2-propanediol (PG), diethylene glycol (DEG), 1,4-butanediol (BDO), ethylene glycol (EG), 1,4-dioxane, ethanol, dichloromethane, and pyridine were of analytical purity. Silane (BSTFA-TMCS, 99:1) and potassium bromide were both of chromatographic purity. All solvents were purchased from Sinopharm Chemical (Shanghai, China). The main physicochemical characteristics of PG, DEG, BDO, and EG were shown in Table 2.

Table 2. The Main Physicochemical Characteristics of the Liquefying Agents

Solvents	Colour	Character	Melting point /° C	Boiling point / ° C	Flash point /° C	Relative density (20 ° C) /g • mL^{-1}	pH	Chemical property	Toxicity
EG	Colorless	Oily liquid	-12.9	197.3	111	1.115	6.0-7.5	Esterification Etherification Substitution Reducibility	Middle
DEG	Colorless	Oily liquid	-10.5	245.0	143	1.118	5.5-7.0	Esterification Etherification Substitution Reducibility	Low
BDO	Colorless	Oily liquid	20.2	228.0	121	1.017	7.0-8.0	Esterification Etherification Substitution Reducibility	Middle
PG	Colorless	Oily liquid	-59.0	188.2	107	1.037	6.0-8.0	Esterification Etherification Substitution Reducibility	Low

Corn Stalk Liquefaction

The scheme of the liquefaction procedure is illustrated in Fig. 1. In the high-pressure reactor (PARR 4848, Champaign, IL, USA), corn stalk (20- to 80-mesh) was liquefied using various diols with phosphoric acid as catalyst under atmospheric pressure. The conditions for liquefaction were as follows: liquid-solid ratio 5:1, catalyst dosage 10%, reaction time 60 min, and reaction temperature 130 to 190 °C. After a preset time, the temperature of the reaction kettle was reduced to 30 °C by the cooling water.

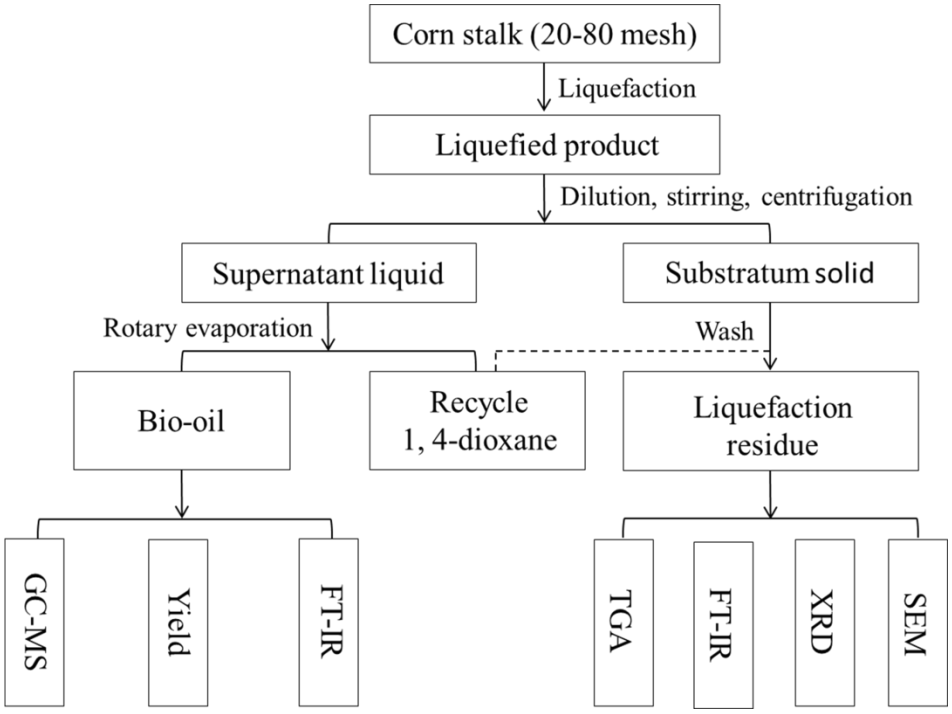

Fig. 1. The treatment flow of products was prepared by liquefaction

Measurement of the Liquefaction Yield

The resultant was diluted with an amount of 1,4-dioxane in excess of 80%, which was recommended as a universal diluent for liquefied biomasses (Yao *et al.* 1994). The diluted product was transferred to a beaker and stirred for 30 min. Subsequently, the mixture was separated into residue and filtrate with a TGL-20M high-speed refrigerated centrifuge at 10,000 rpm and 10 °C for 15 min. After centrifugation, the liquefaction product (bio-oil) was prepared after the organic solvent was removed from the supernatant using rotary evaporation at 40 °C. The residue was thoroughly rinsed with recycled 1,4-dioxane and dried in an oven at 105 ºC for 24 h. The residue rate was defined as the percent dry weight of the dioxane insoluble substance to the total charged lignocellulosic biomass, and it was usually used as an index of the extent of liquefaction (Yamada and Ono 1999). The residue and liquefaction rates were calculated as shown in Eqs. 1 and 2. The residue quality was defined as the dry weight of the dioxane insoluble substance. The corn stalk quality was defined as the dry weight of corn stalks which were initially put into a high-pressure reactor.

$$\text{Residue yield} = \text{residue quality/corn stalk quality} \times 100\% \quad (1)$$

$$\text{Liquefaction yield} = 1 - \text{residue yield} \quad (2)$$

Analysis Methods

GC-MS analysis

For the silanization reaction, 20 mL of the filtrate was extracted with 10 mL of dichloromethane. The extract was dried and 2 mL of dichloromethane was added to dissolve the dry extract. Subsequently, 50 µL of dissolved extract was pipetted into a 1.5 mL vial, which was placed in a vacuum drying oven at 40 °C for 30 min. Finally,

silanization took 45 min at 70 °C after adding 80 μL of pyridine and 150 μL of BSTFA-TMCS as silylating agents.

For gas chromatography (GC), an RTX-5MS (30 m × 0.25 mm × 0.25 μm) column (Agilent, Palo Alto, USA) was used. The flow rate of the highly pure helium carrier gas and the purge flow were 1 and 3 mL/min, respectively. The split ratio was 10:1. A total of 0.2 μL of sample was injected to the inlet at 300 °C for 3 min solvent delay. The temperature program of the column was as follows: initial temperature of 80 °C for 3 min, raised to 150 °C at 5 °C/min, and immediately raised to 300 °C at 10 °C/min. The temperature was maintained at 300 °C for 5 min. The total operation time was 37 min.

The mass spectrometry (MS) conditions were as follows. The temperatures of the interface and ion source were 220 and 200 °C, respectively. Mass scanning ranged from 40 to 1000 in the electron impact mode.

The main components of the treated bio-oil were characterized using GC-MS (Agilent, Palo Alto, CA, USA).

FTIR analysis

FTIR spectra were recorded using a VERTEX 70 spectrometer (Bruker Optics, Karlsruhe, Germany), with a wavelength range of 4000 to 400 cm^{-1}. Sixteen scans at a 4 cm^{-1} resolution were averaged and referenced against air. Before scanning, transparent films were prepared from the sample and KBr with a 1:100 (w/w) ratio.

Thermogravimetric analysis

A 10-mg sample (corn stalk and liquefaction residues) was heated to a final temperature of 800 °C at a heating rate of 20 °C/min using a thermogravimetric analyzer (TGA-Q50, Shimadzu, Kyoto, Japan) under nitrogen protection.

XRD analysis

The XRD patterns of the liquefaction residue samples were compared using a Lab XRD-6100 diffractometer (Shimadzu) with a Ni-filtered Cu Kα-radiation at 40 kV and 50 mA. Powder samples were exposed to X-rays at a 4 °/min scan rate in the 2θ range of 5 to 40°. The relative crystallinity (Crl) of the polymers was calculated by dividing the area of the crystalline peaks by the total area under the curve (Abdou *et al.* 2008).

SEM analysis

The surface morphology of the corn stalk and liquefaction residues obtained using PG was carried out utilizing a scanning electron microscope (JSM-IT300, JEOL, Tokyo, Japan). Before the investigations, the surfaces of the samples were covered in gold to confer them electrical conductivity.

RESULTS AND DISCUSSION

Effect of Temperature on the Liquefaction Experiment

The "competition" between cleavage and condensation always occurred during the liquefaction of corn stalks. The cleavage reaction mainly occurred in the early stage of liquefaction, while polycondensation had a predominant role in the later stage. The reversal was affected by the type of raw material and the reaction conditions to a large

extent (Zhang and Zhao 2014). However, under relatively mild reaction conditions, the liquefaction reaction was preferred over the condensation of the liquefied products (Liu *et al.* 2012).

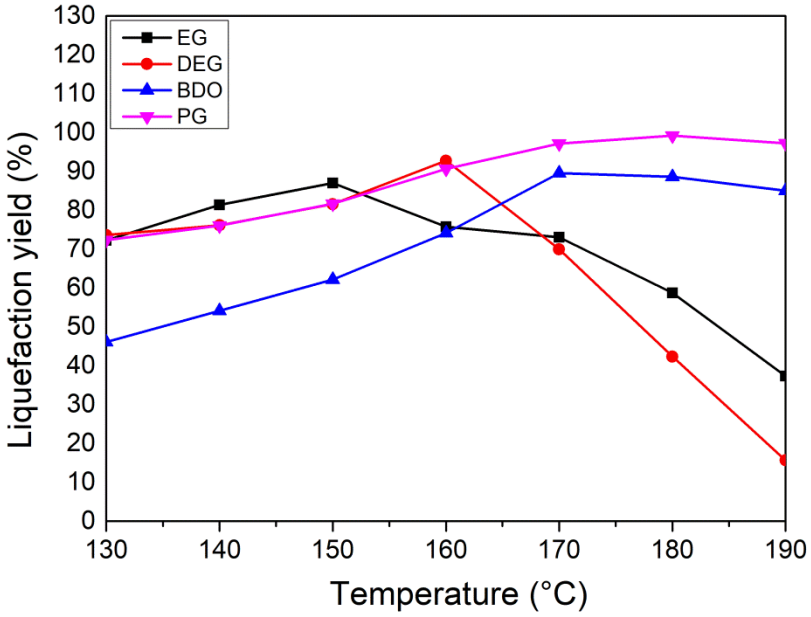

Fig. 2. Effect of reaction temperature on liquefaction yield of bio-oil was prepared by EG, DEG, BDO, and PG, respectively

As can be seen from Fig. 2, the liquefaction yields were 99.2, 89.5, 92.7, and 87.0% when PG, DEG, BDO, and EG were used as liquefaction agents under the optimum reaction temperatures of 180, 170, 160, and 150 °C, respectively. Reaction temperature influenced the liquefaction yield. When the temperature increased from 130 °C to the optimum temperature of each group, the liquefaction yield of the four groups was increased significantly. The reason was that the reaction medium gradually infiltrated the microstructure of the main component of corn stalk to destroy the intermolecular connection and degrade some cellulose molecules during the liquefaction process. The reaction rate reached a maximum and the liquefaction reaction was the fastest when the optimum temperature was reached. However, when the temperature was further increased, the liquefaction yield decreased. This was attributed to polymerization being prominent under the higher temperature and acidity conditions in the liquefied system. Initially, the biomass was decomposed and depolymerized into small molecular compounds, which could concentrate and polymerize into new compounds. Therefore, the residue yield was going up, which illustrated that the high temperature was not conducive to the catalytic liquefaction of corn stalks. With consideration, the samples (residue and bio oil) which were obtained at the 180, 170, 160, and 150 °C using PG, DEG, BDO, and EG, respectively, were used for later performance analyses.

GC-MS Analysis of the Bio Oil

Hyphenated techniques such as GC-MS are very suitable methods to analyze complex mixtures and to identify individual components. The total ion chromatograms (TICs) of the four types of bio-oil were exhibited in Fig. 3.

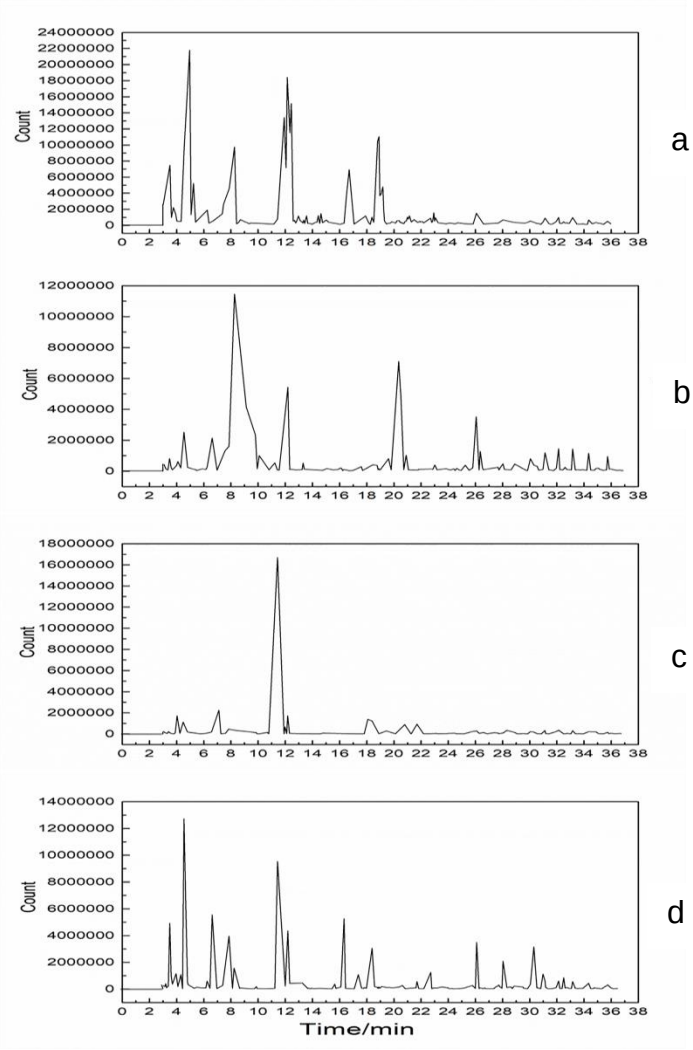

Fig. 3. GC-MS total ion chromatogram of concentrate: a) prepared with PG; b) prepared with BDO; c) prepared DEG; d) prepared with EG

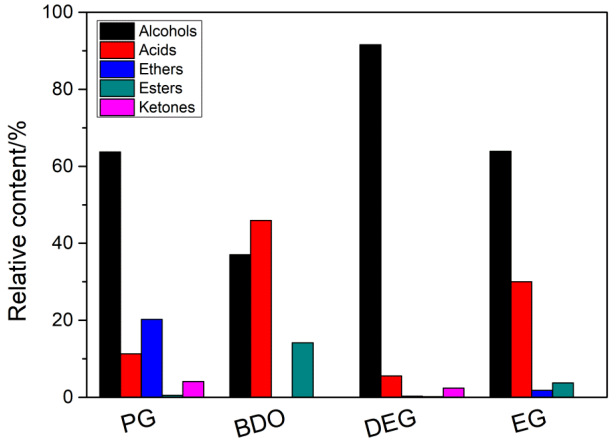

Fig. 4. Relative contents distribution of the different liquefied organic substance

The results indicated that the types and contents of the products were completely different after the treatment using different liquefaction agents. There were significant differences in the peak distributions of the four spectra. Moreover, the peak heights of the same species were different, which showed that the different liquefaction agents had a great impact on the composition and distribution of the bio-oil (Liu and Zhang 2008; Fan *et al*. 2011). The ratio of each TIC showed unique features. The ratios of the organic species were 52, 50, 31, and 53, and could be associated with the treatment using PG, BDO, DEG, and EG respectively. The definite distribution determined using the area normalization method was shown in Fig. 4.

Table 3. Comparison of Main Chemical Components of Four Kinds of Bio-oil

Compound Name	Relative Peak Area (%)			
	PG	BDO	DEG	EG
Ethanol	1.243	2.725	-	0.307
Ethylene glycol	5.941	5.482	3.425	27.614
1,2-Propanediol	30.043	-	0.705	0.262
2-n-propyl-propane-1,3-diol	2.015	-	-	-
2-Methyl-1-propanol	0.526	-	-	0.090
sec-Butanol	0.973	-	-	-
Diethylene glycol	0.338	0.177	76.386	20.743
1, 2-Butanediol	7.175	0.286	-	-
2,3-Butanediol	3.920	-	-	0.118
Pinacol	6.211	0.803	0.070	-
4-Methyl-3-heptanol	0.695	-	-	-
Nonaethyleneglycol	0.229	0.722	-	-
3,6,9,12,15,18,21, 24,27,30-Decaoxadotriacontane-1,32-diol	-	0.740	-	0.359
3-Hydroxy-1,5-hexadiene	-	0.436	-	1.591
1,4-Butylene glycol	-	7.939	-	-
3-Methyl-1-cyclohexen-1-ol	-	2.024	0.124	-
Glycerol	-	0.236	0.270	1.300
3-Buten-1-ol	-	1.350	-	-
Tetraethylene glycol	-	10.959	4.172	0.382
4-(tert-Butoxy)butanol	-	0.725	-	-
3,7,11-Trioxate-tradecane-1,14-diol	-	0.697	-	-
Triethylene glycol	-	-	3.997	7.413
Hexaoxy ethylene glycol	-	-	1.248	0.238
Propyl alcohol	-	-	-	1.496
Lactic acid	0.672	2.481	0.238	1.029
Levulinic acid	4.757	29.320	1.380	3.153
(2-{2-[2-(2-Acetoxy-ethoxy)-ethoxy]-ethoxy}-ethoxy)-acetic acid	0.121	-	2.488	1.016
(R)-(-)-5-Oxo-2-Methyl-2-tetrahydro-furancarboxylic acid	2.945	10.436	0.148	11.361
Palmitic acid	0.587	-	0.774	5.175
Stearic acid	0.218	0.709	0.244	3.308
3-Methyl-2-furoic acid	-	1.064	-	-
Linoleic acid	-	0.123	-	0.515

Oxalic acid	-	-	-	0.771
Methacrylic acid	-	-	-	0.902
Tripropyleneglycol methyl ether	19.458	-	0.118	0.192
1-(2-Butoxy-1-methylethoxy)-2-propanol	0.572	-	-	-
2(2-Ethoxyethoxy)ethanol	-	-	-	1.618
Glycerin fatty acid ester	0.233	0.259	-	1.808
alpha-Monostearin	0.292	0.372	-	1.532
2-hydroxy-3-methyl propyl acetate	-	6.129	-	-
Palmitic acid, ester with 1, 4- butanediol	-	6.092	-	-
3-Hydroxy-propionic acid 2-(2-carboxy-eth-oxycarbonyl)-ethyl ester	-	1.318	-	-
m-Ethylphenol	0.169	1.104	-	0.134
3-Hydroxy-2-butanone	3.647	-	-	-

Note: this only showed the peak area of the compound group, which was more than 0.500%; - indicating that there was no such compound.

Results in Table 3 show that when different liquefying agents were used, the chemical composition of the bio-oil liquefaction products also exhibited certain differences. Each type of bio-oil has its own unique composition, but the main components belong to the same chemical species (organic acids, alcohols, ethers, esters, ketones, aldehydes, and phenols). As shown in Fig. 4, there were some differences in the contents of the main chemical species for the four types of bio-oil. When PG was the chosen liquefaction agent, the main liquefaction products were alcohols and ethers, and their relative contents were 63.7 and 20.3%, respectively. However, no aldehydes were produced. Organic acids and alcohols (46.0 and 37.0%) were the essential products of the BDO liquefaction reaction, but no ethers and ketones were generated. Furthermore, 91.6% alcohols were detected in the liquefaction products when DEG was the liquefying agent, while no aldehydes were detected. The percentage of alcohols was the highest after the liquefaction using EG, while the percentage of organic acids was slightly smaller than that of the alcohols. Their relative contents were 63.9 and 30.0%, respectively. However, ketones were not detected. At the same time, small amounts of esters and phenols were discovered in all four types of bio-oils. Liquefied products rich in hydroxyl groups could have direct applications in agriculture and the production of industrial membranes, polyurethane foam, and polyurethane adhesive.

When using different liquefying agents, the chemical composition of the liquefied bio-oil generated by the same raw materials displayed some similarities. However, the chemical substances composing the bio-oils and their respective amounts were different, and so were their molecular weights. According to production necessities, the desired product can be obtained using separation and purification methods such as fractional extraction, thin layer chromatography (TLC) (Garcia-Perez *et al.* 2007), *etc*.

FTIR Spectrum Analysis of the Bio Oil

Figure 5 showed the position of IR absorption bands of corn stalk and four types of liquefied bio oils. The strong bands at 3419 cm^{-1} for all of the samples were assigned to the O-H stretching vibrations for the phenolic and alcohol compounds. Namely, the signal might be the hydroxyl of the aliphatic chain of the carbohydrate, the phenolic hydroxyl of the benzene ring in lignin, the alcohol hydroxyl of the branched chains connected to the benzene ring, or the alcohol hydroxyl of the residual liquefaction agent.

In addition, the absorption peak intensities of the four types of liquefied products were significantly weaker than that of corn stalk. This was ascribed to the condensation reaction between the hydroxyl groups in the liquefied corn stalk and the acid catalyst and alcohols liquefier to produce water or other small molecules (Yamada and Ono, 1999). C-H stretching of alkanes at 2908 cm^{-1} could also be observed for all of the samples.

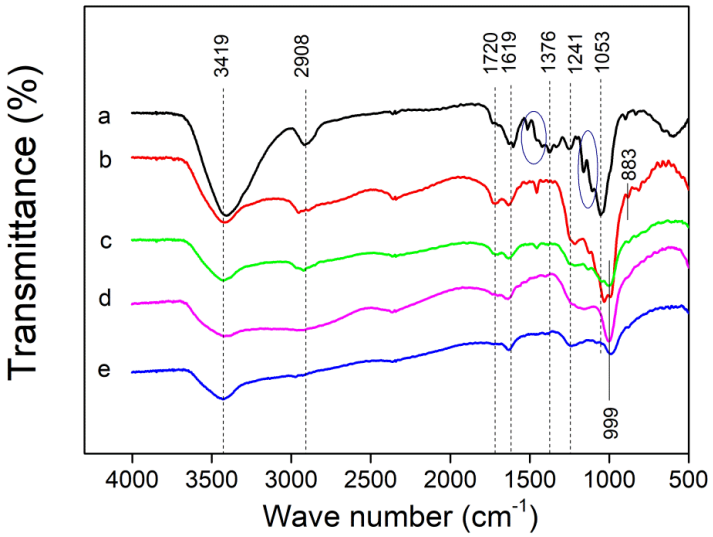

Fig. 5. FTIR spectra of corn stalk and bio oils: a) represents corn stalk; b) represents liquefaction product with EG; c) represents liquefaction product with DEG; d) represents liquefaction product with BDO; e) represents liquefaction product with PG

Several other signals were identified: the carbonyl of carbohydrates at 1720 cm^{-1}, C–H bending vibration at 1376 cm^{-1} (the characteristic absorption peak of cellulose), methoxyl of guaiacyl at 1241 cm^{-1}, and the C–O single bond of the $–CH_2OH$ group in corn stalk at 1053 cm^{-1}. The signal positions of the four types of liquefied oils at 1053 cm^{-1} were offset by the corn stalk. It is possible that the degradation of the three major components of the raw material might have caused changes of substituents in the products. The signal observed at 1720 cm^{-1} corresponded to the C=O stretching vibration agreeable with the existence of ketone, aldehyde, carboxylic, and esters groups. This indicated that the liquefied oils contained of many unsaturated oxygenated compounds, most of which were the degradation products of holocellulose. There was a significance peak at 1300-950 cm^{-1} in the oil products, corresponding to the C-O stretching and O-H bending of the primary, secondary and tertiary alcohols.

Compared with the intensity of the signals for corn stalk, the intensity of the absorption peaks of the liquefied products weakened or even disappeared at 1720 to 1376 cm^{-1} and 1241 to 1053 cm^{-1}. This was mainly ascribed to the formation of new substances due to the degradation of the lignin molecules and the gradual decrease in late liquefaction of the diols liquefaction agents.

There was a vibration absorption peak at 883 cm^{-1}, which was characteristic of β-glucosidic linkages between the sugar units. Compared with the EG liquefaction oil, the signal intensity of the other three types of products weakened or even disappeared. This may have been due to the involvement of carbohydrates in the chemical reaction

generating insoluble 1,4-dioxane. The results showed that after liquefaction, the three main components were degraded, and the liquefied products contained a variety of active functional groups, which could be further processed and used as energy sources or high value materials (Yu *et al.* 2006a).

FTIR Spectrum Analysis of the Liquefaction Residue

All IR spectra of the raw material and the residues presented strong peaks at 3410 cm^{-1} (Fig. 6). These were attributed to the stretching vibration of O–H (Schwanninger *et al.* 2004). This implied that hydroxyl compounds existed in both the raw material and residue. However, compared with the raw material curve, the residues peak were significantly reduced, which indicated that during liquefaction, the amount of hydroxyl in the residue decreased due to the changes of the hydroxyl groups. The signals of 2917 cm^{-1} in corn stalk and all the residues were caused by the methyl and methylene C–H bond stretching vibration (Vázquez *et al.* 1997). The 1373, 1051, and 1156 cm^{-1} signals were the characteristic absorption peaks of cellulose and hemicellulose. Compared with the raw material curve, the other four groups in the three peak curve were weaker or even disappeared, which showed that most of the cellulose and hemicellulose in corn stalk was liquefied, but not completely, during the liquefaction process. At 1722 cm^{-1}, the uncoupling C=O stretching vibration was mainly the absorption peak of ketones, esters, and saccharides from the cellulose and hemicellulose of corn stalk (Hoareau *et al.* 2011). The absorption peak of the four residues was transferred to 1629 cm^{-1} and the intensity increased obviously, probably due to the decomposition of ketones or esters in cellulose and hemicellulose.

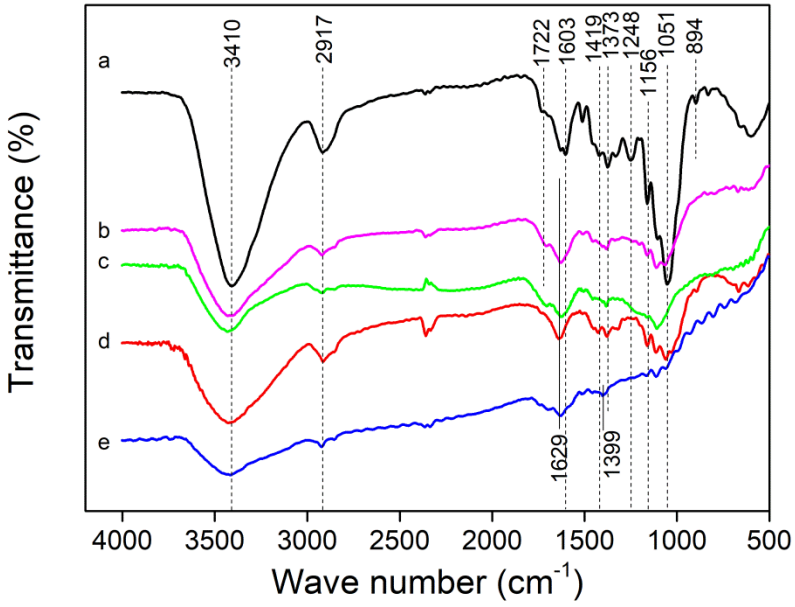

Fig. 6. Comparison of corn stalk and liquefaction residues: a) described corn stalk; b) described as liquefaction residue with DEG; c) described as liquefaction residue with PG; d) described as liquefaction residue with EG; e) described as liquefaction residue with BDO

Compared with the corn stalk, the band assigned to the stretching vibrations of glucosidic bond of residues at 894 cm^{-1} distinctly weakened or even disappeared after the liquefaction process, which confirmed carbohydrates were significantly changed. The C–H bending vibration was expressed at 1419 cm^{-1}, while all the residues almost

disappeared at this wavenumber, which illustrated that the liquefaction process changed the methyl and ethylene groups of the raw materials. The 1511 cm^{-1} peak, attributed to the stretching vibration of the carbon atoms in the aromatic benzene ring, was the characteristic peak of lignin, while at 1248 cm^{-1} was the characteristic signal of the lilac ring (Pan *et al.* 2010). The peak multiplicity at 1248 cm^{-1} was a representative signal of the p-hydroxyphenyl structures of herbage lignin (Sun *et al.* 2000). These signals were notably decreased and disappeared for all the residues indicating that the lilac ring of lignin disappeared, while the benzene ring was reduced but still existed in the residues. The characteristic peaks under 1200 cm^{-1} were more complex and might have been caused by the deformation vibrations of the C–H, C–O, and C–C bonds.

In a word, the IR spectra of the liquefaction residue reported that the functional groups of cellulose, hemicellulose and lignin were disappeared and the liquefaction degree of lignin was the largest.

TGA Analysis of the Liquefaction Residue

As seen in Fig. 7, the thermal weight loss of corn stalk and the four types of residue exhibited different behaviors under the same conditions. The pyrolysis process can be divided into three stages: heating, rapid weight loss, and slow weight loss.

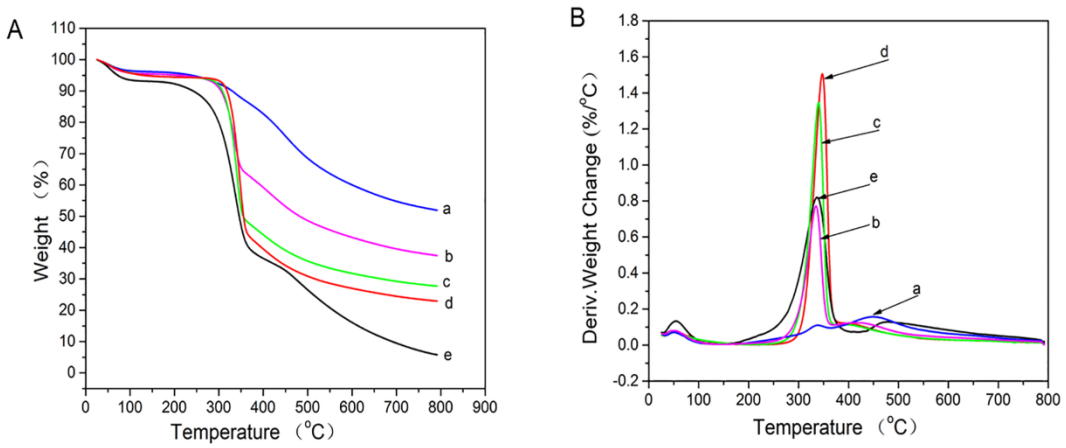

Fig. 7. TG curves (A) and DTG curves (B) of raw material and residues: a) was on behalf of liquefaction residue with PG; b) was on behalf of liquefaction residue with DEG; c) was on behalf of liquefaction residue with BDO; d) was on behalf of liquefaction residue with EG; e) was on behalf of corn stalk

During the first stage of corn stalk decomposition a large amount of the free water content of corn stalk was lost. The second stage involved a significant weight loss. Some internal restructuring also occurred at this stage. The modification of the raw materials would release small molecular weight compounds, such as H_2O, CO, CO_2, *etc*. In addition, a large amount of cellulose and hemicelluloses decomposed. Moreover, lignin softened and decomposed, and carbon and volatile substances also formed. The decomposition of cellulose and hemicellulose produced mostly volatiles, while the decomposition of lignin generated mainly carbon. The decomposition during the third stage was very slow, and the associated mass loss was much smaller than that in the second stage. At this stage, the mass loss was considered to be caused by the further volatilization of carbon through fracturing the C–C and C–H bonds.

In the first stage, where temperature was increased from initial temperature to 150 °C, compared with the stable thermal weight loss of the four types of residue, the mass loss of corn stalk was obviously due to degradation of the small molecular substances in the corn stalk or the loss of moisture.

During the second stage, the critical range of thermal weight loss was reached in the 150 to 550 °C temperature range. Figure 7 (A) shows that the percentage of decomposition of the liquefaction residue with EG was smaller than that of corn stalk in the second stage, which meant that the cellulose and hemicellulose content in the residue was reduced, resulting in a lower percentage of decomposition. This was similar to the residue of the BDO liquefaction during the second stage decomposition. The mass loss of liquefaction residue using DEG was less than the one obtained when BDO was the liquefying agent. As already mentioned, cellulose and hemicellulose were still found in the residue, and the liquefaction reaction was incomplete. The curves of the residue obtained from PG liquefaction showed that the weight loss curve of cellulose disappeared, and only other slow decomposing substances remained. These might have been the residual lignin and a number of large molecular substances, which exhibited fractures of the C–C and C–H bonds in the TGA, that reassembled after cracking. As shown in Fig. 7 (B), all the thermal weight loss for the five types of substances reached peak points at temperatures between 150 and 375 °C because volatile and small organic molecules can be degraded in this temperature range. However, the nonvolatile macromolecular substances degraded at temperatures between 375 and 550 °C.

During the last stage (550 to 800 °C), the TG curve showed a constant tendency, since pyrolyzation was almost completed and the waste from the five types of materials were ash and carbon that could not be degraded. When the temperature reached 800 °C, the final extents of weight loss were 95, 77, 72, 62, and 49% for corn stalk, EG, BDO, DEG, and PG, respectively. This happened because biomass was composed of cellulose, hemicellulose, and lignin, whose contents could evidently impact the pyrolyzation of biomass. After the pyrolyzation of biomass, carbohydrates were pyrolyzed to evaporable materials, while carbon was the mainly pyrolysis product (Antal and Varhegyi 1995; Yan *et al*. 2005; Sonobe and Tanthapanichakoon 2007). There were less than three main materials in the residue obtained after liquefaction; therefore its thermal weight loss was smaller.

To sum up, by comparing the TGA data of the four residues, the order of their thermal stability was EG < BDO < DEG < PG. The main reason for this was that biomass is mainly composed of three major components, and their contents had a great influence on the pyrolysis of biomass. The thermal weight loss rate of the residue of the PG liquefaction was the smallest of all analyzed residues. This indicated that the three components of corn stalk were basically completely liquefied and also proved that the best liquefaction agent was PG in this study.

XRD Analysis of the Corn Stalk and Liquefaction Residue

The XRD spectra of untreated and treated corn stalk samples were presented in Fig. 8. There were two broad peaks at 15 and 22° for corn stalk, which were consistent with the cellulose I lattice (Cheng *et al.* 2011). The cellulose I lattice was preserved in the liquefaction residue when EG or DEG was used as liquefaction agent. Although the main peak position remained roughly the same for these two samples, there were noticeable shifts of the secondary peak from 15.6 to 14.6° for the DEG treatment, and of the main peak from 21.9 to 22.4°, when using EG liquefaction. The Crls of the untreated, EG, and

DEG treated samples were 61.4, 82.4, and 60.3%, respectively. Depending on the liquefaction of an amorphous area of cellulose, the CrI of the residue from the EG liquefaction process was higher compared to the untreated or the DEG treated samples. The broad peaks of the residue of DEG liquefying were obviously weakened, indicating that the crystalline area of cellulose was damaged to a certain extent, and the degree of liquefaction of cellulose in this residue was better than the one obtained with EG. The two types of liquefying agents (PG and BDO) disappeared at the two diffraction peaks, forming "amorphous" cellulose. This was attributed to the crystalline structure of cellulose and hemicellulose being completely destroyed by the catalyst and high temperature, and the cracking of the cellulose molecules. Furthermore, this demonstrated that the degree of cellulose liquefaction was quite high and cellulose was almost completely liquefied.

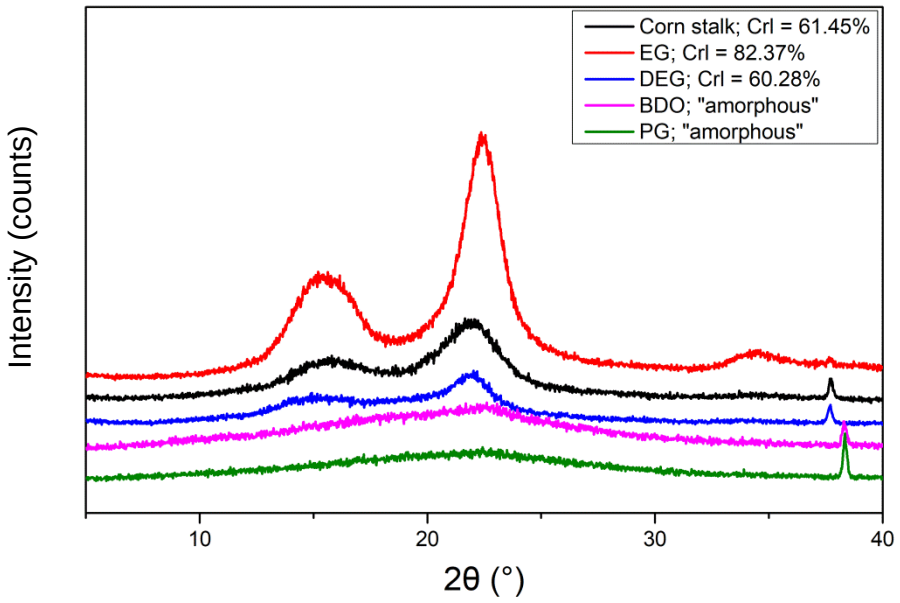

Fig. 8. X-ray diffraction patterns of corn stalk and liquefaction residues were prepared by EG, DEG, BDO, and PG, respectively.

SEM Analysis of the Corn Stalk and Liquefaction Residue

Morphological changes of the corn stalk before and after liquefaction using PG were observed via SEM. Figure 9 (a1)–(a3) displayed the surface morphology of the raw material magnified 250, 500, and 1000 times, respectively. It can be observed from this figure that the corn stalk has fibrous and compact structure. From Fig.9 (a3), there were clear gaps between the corn stalk layer and the layer to be observed. Under this condition, solvent could diffuse easily inside tissue of the corn stalk during the liquefying process, which notably improved the reaction effect.

Figure 9 (b1)–(b3) shows the morphological structure after liquefaction magnified 250, 500, and 1000 times, respectively. The surface structure of the liquefied residue and the corn stalk was completely different compared to the raw material. The close cladding structure of lignin, cellulose, and hemicellulose was notably damaged, and the degree of polymerization was reduced. The surface of the residue was rough, irregular, and granulated. Moreover, the residues were not cross linked to each other and became loose

(Pan *et al*. 2007). Char might be produced from the condensation of lignin and plant fiber. It was indicated that the fiber structure of the liquefied corn stalk was destroyed and basically liquefied. Figure 9 (b3) showed there were clear pores and a large specific surface area on the surface of the residue, indicating that the residue contained high quality activated carbon.

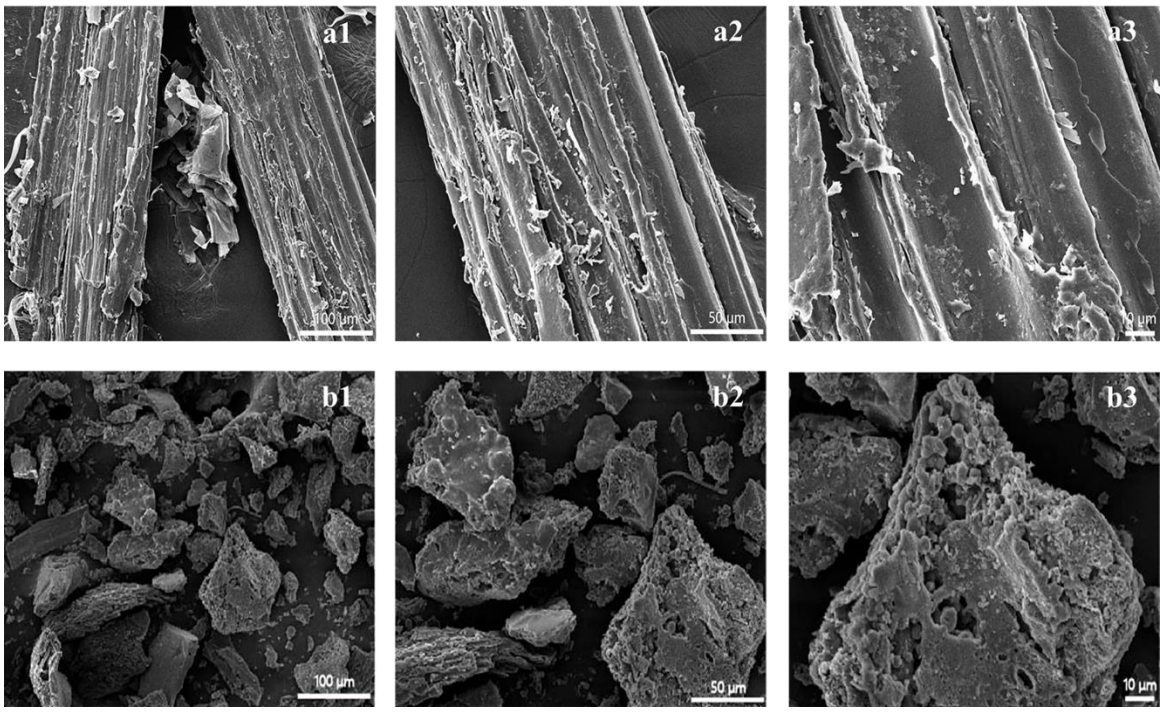

Fig. 9. SEM photographs of corn stalk and liquefied residue: a was corn stalk, a1(250x), a2(500x), a3(1000x); b was liquefaction residue with PG, b1(250x), b2(500x), b3(1000x)

CONCLUSIONS

1. The order of conversion efficiency of diol liquefying agents at respectively optimum reaction temperature was 1,2-propanediol (PG) > 1,4-butanediol (BDO) > diethylene glycol (DEG) > ethylene glycol (EG). In addition, the costs of PG, DEG, and EG were similar and were approximately half the cost of BDO.
2. For the new liquefying agents (PG, DEG, and BDO), the liquefaction of corn stalk, degradation of corn stalk, main components, and functional groups of the liquefied products and residues were confirmed by GC-MS and FT-IR. The results were very similar to those of the traditional EG liquefaction. The results of the GC-MS analysis showed that the composition of corn stalk bio-oil was complex, containing organic acids, ketones, alcohols, ethers, aromatic compounds, aldehydes, and esters. However, the relative content of each component was very different after processing with the different liquefying agents. Furthermore, analyzing and comparing the FTIR images of the corn stalk and liquefaction products demonstrated that a large number of hydroxyl groups were generated during liquefaction. Therefore, the product of PG liquefied lignocellulose was considered to be very similar to that of the current diols liquefaction process.

3. Using TGA analysis it was determined that the order of thermal stability for the residue was EG < BDO < DEG < PG when these four types of polyols were liquefying agents. This was due to the notable impact of the content of the component on the pyrolysis of the biomass. Meanwhile, biomass was mainly composed of cellulose, hemicellulose, and lignin. The liquefaction residue was characterized using XRD, SEM, and FTIR, which allowed the analysis of the effect of several solvents on liquefaction. Considering the effect and cost of liquefaction, PG was the most suitable liquefaction agent for this study compared with DEG, EG, and BDO.

ACKNOWLEDGMENT

This project was financially supported by the National Key R&D Program China (No.2017YFB0308300) and the National Nature Science Foundation of China (NSFC, No.21576213, 31270631).

REFERENCES CITED

Abdou, E. S., Nagy, K. S., and Elsabee, M. Z. (2008). "Extraction and characterization of chitin and chitosan from local sources," *Bioresource Technology* 99(5), 1359-1367. DOI: 10.1016/j.biortech.2007.01.051

Alma, M. H., Yoshioka, M., Yao, Y., and Shiraishi, N. (1998). "Preparation of sulfuric acid-catalyzed phenolated wood resin," *Journal of Polymer Engineering* 32(4), 297-308. DOI: 10.1007/BF00702897

Antal, M. J., and Varhegyi, G. (1995). "Cellulose pyrolysis kinetics: The current state of knowledge," *Ind. Eng. Chem. Res.* 34(3), 703-717. DOI: 10.1021/ie00042a001

Breunig, M., Gebhart, P., Hornung, U., Kruse, A., and Dinjus, E. (2017). "Direct liquefaction of lignin and lignin rich biomasses by heterogenic catalytic hydrogenolysis," *Biomass & Bioenergy* 111, 352-360. DOI: 10.1016/j.biombioe.2017.06.001

Cheng, G., Varanasi, P., Li, C., Liu, H., Melnichenko, Y. B., Simmons, B. A., Kent, M. S., and Singh, S. (2011). "Transition of cellulose crystalline structure and surface morphology of biomass as a function of ionic liquid pretreatment and its relation to enzymatic hydrolysis," *Biomacromolecules* 12(4), 933-41. DOI: 10.1021/bm101240z

Demirbaş, A. (2001). "Biomass resource facilities and biomass conversion processing for fuels and chemicals," *Energy Conversion & Management* 42(11), 1357-1378. DOI: 10.1016/S0196-8904(00)00137-0

Fan, S. P., Zakaria, S., Chia, C. H., Jamaluddin, F., Nabihah, S., Liew, T. K., and Pua, F. L. (2011). "Comparative studies of products obtained from solvolysis liquefaction of oil palm empty fruit bunch fibres using different solvents," *Bioresource Technology* 102(3), 3521-3526. DOI: 10.1016/j.biortech.2010.11.046

Field, C. B., Campbell, J. E., and Lobell, D. B. (2008). "Biomass energy: The scale of the potential resource," *Trends in Ecology & Evolution* 23(2), 65-72. DOI: 10.1016/j.tree.2007.12.001

Garcia-Perez, M., Chaala, A., Pakdel, H., Kretschmer, D., and Roy, C. (2007). "Characterization of bio-oils in chemical families," *Biomass & Bioenergy* 31(4), 222-242. DOI: 10.1016/j.biombioe.2006.02.006

Hatfield, R., and Vermerris, W. (2001). "Lignin formation in plants. The dilemma of linkage specificity," *Plant Physiology* 126(4), 1351. DOI: 10.1104/pp.126.4.1351

Hoareau, W., Trindade, W. G., Siegmund, B., Castellan, A., and Frollini, E. (2011). "Sugar cane bagasse and curaua lignins oxidized by chlorine dioxide and reacted with furfuryl alcohol: Characterization and stability," *Polymer Degradation & Stability* 86(3), 567-576. DOI: 10.1016/j.polymdegradstab.2004.07.005

Kobayashi, M., Hatano, Y., and Tomita, B. (2001). "Viscoelastic properties of liquefied wood/epoxy resin and its bond strength," *Holzforschung* 55(6), 667-671. DOI: 10.1515/HF.2001.108

Kunaver, M., Medved, S., Cuk, N., Jasiukaityte, E., Poljansek, I., and Strnad, T. (2010). "Application of liquefied wood as a new particle board adhesive system," *Bioresource Technology* 101(4), 1361-8. DOI: 10.1016/j.biortech.2009.09.066.

Lee, S. H., Yoshioka, M., and Shiraishi, N. (2015a). "Liquefaction and product identification of corn bran (CB) in phenol," *Journal of Applied Polymer Science* 78(2), 311-318. DOI: 10.1002/1097-4628(20001010)78:23.0.CO;2-N

Lee, S.H., Yoshioka, M., and Shiraishi, N. (2015b). "Liquefaction of corn bran (CB) in the presence of alcohols and preparation of polyurethane foam from its liquefied polyol," *Journal of Applied Polymer Science* 78(2), 319-325. DOI: 10.1002/1097-4628(20001010)78:2<319::AID-APP120>3.0.CO;2-Z

Liu, Y., Wang, Y., Ruan, R., Li, Z., Lin, X., and Liu, C. (2012). "Optimization of processing parameters for rapid liquefaction of corn stover under atmospheric pressure," *Nongye Jixie Xuebao/transactions of the Chinese Society of Agricultural Machinery* 43(8), 110-115. DOI: 10.6041/j.issn.1000-1298.2012.08.021

Liu, Z., and Zhang, F. S. (2008). "Effects of various solvents on the liquefaction of biomass to produce fuels and chemical feedstocks," *Energy Conversion & Management* 49(12), 3498-3504. DOI: 10.1016/j.enconman.2008.08.009

Minowa, T., Fang, Z., Ogi, T., and Varhegyi, G. (2004). "Decomposition of cellulose and glucose in hot-compressed water under catalyst-free conditions," *Journal of Chemical Engineering of Japan* 31(1), 131-134. DOI: 10.1252/jcej.31.131

Minowa, T., Kondo, T., and Sudirjo, S. T. (1998). "Thermochemical liquefaction of Indonesian biomass residues," *Biomass & Bioenergy* 14(5), 517-524. DOI: 10.1016/S0961-9534(98)00006-3

Minowa, T., Zhen, F., Ogi, T., and Várhegyi, G. (1997). "Liquefaction of cellulose in hot compressed water using sodium carbonate: Products distribution at different reaction temperatures," *Journal of Chemical Engineering of Japan* 30(1), 186-190. DOI: 10.1252/jcej.30.186

Nikolić, S., Mojovic´, L., Rakin, M., Pejin, D., and Savić, D. (2008). "A microwave-assisted liquefaction as a pretreatment for the bioethanol production by the simultaneous saccharification and fermentation of corn meal," *Chemical Industry & Chemical Engineering Quarterly* 14(4), 231-234. DOI: 10.2298/CICEQ0804231N

Pan, H., Shupe, T. F., and Hse, C. Y. (2010). "Synthesis and cure kinetics of liquefied wood/phenol/formaldehyde resins," *Journal of Applied Polymer Science* 108(3), 1837-1844. DOI: 10.1002/app.27756

Pan, H., Shupe, T. F., and Hse, C. Y. (2007). "Characterization of liquefied wood residues from different liquefaction conditions," *Journal of Applied Polymer Science* 105(6), 3740-3746. DOI: 10.1002/app.26435

Pu, S., and Shiraishi, N. (1993a). "Liquefaction of wood without a catalyst II. Weight loss by gasification during wood liquefaction, and effects of temperature and water," *Journal of the Japan Wood Research Society* 39(4) 453-458.

Pu, S., and Shiraishi, N. (1993b). "Liquefaction of wood without a catalyst. 1: Time course of wood liquefaction with phenols and effects of wood/phenol ratios," *Journal of the Japan Wood Research Society* 39(4), 446-452.

Pu, S., and Shiraishi, N. (1994). "Liquefaction of wood without a catalyst IV. Effect of additives, such as acid, salt, and neutral organic solvent," *Mokuzai Gakkaishi* 40(8), 824-829.

Saidur, R., Abdelaziz, E. A., Demirbas, A., Hossain, M. S., and Mekhilef, S. (2011). "A review on biomass as a fuel for boilers," *Renewable & Sustainable Energy Reviews* 15(5), 2262-2289. DOI: 10.1016/j.rser.2011.02.015

Saxena, R. C., Adhikari, D. K., and Goyal, H. B. (2009). "Biomass-based energy fuel through biochemical routes: A review," *Renewable & Sustainable Energy Reviews* 13(1), 167-178. DOI: 10.1016/j.rser.2007.07.011

Schwanninger, M., Rodrigues, J. C., Pereira, H., and Hinterstoisser, B. (2004). "Effects of short-time vibratory ball milling on the shape of FT-IR spectra of wood and cellulose," *Vibrational Spectroscopy* 36(1), 23-40. DOI: 10.1016/j.vibspec.2004.02.003

Shiraishi, N., Shirakawa, K., and Kurimoto, Y. (1996). "Method for preparing a liquefied solution of ligno-cellulose substance with polyhydric alcohols," U.S. Patent No. EP0472474.

Sonobe, T., and Tanthapanichakoon, W. (2007). "Pyrolysis behaviors of rice straw, rice husk, and corncob by TG-MS technique," *Journal of Analytical & Applied Pyrolysis* 78(2), 265-271. DOI: 10.1016/j.jaap.2006.08.002

Stiller, A. H., Dadyburjor, D. B., Wann, J. P., Tian, D., and Zondlo, J. W. (1996). "Co-processing of agricultural and biomass waste with coal," *Fuel Processing Technology* 49(1–3), 167-175. DOI: 10.1016/S0378-3820(96)01051-X

Sun, R. C., Tomkinson, J., Sun, X. F., and Wang, N. J. (2000). "Fractional isolation and physico-chemical characterization of alkali-soluble lignins from fast-growing poplar wood," *Polymer* 41(23), 8409-8417. DOI: 10.1515/hfsg.1997.51.3.244

Tymchyshyn, M., and Xu, C. (2010). "Liquefaction of bio-mass in hot-compressed water for the production of phenolic compounds," *Bioresource Technology* 101(7), 2483-2490. DOI: 10.1016/j.biortech.2009.11.091

Vasilakos, N. P., and Austgen, D. M. (1985). "Hydrogen-donor solvents in biomass liquefaction," *Industrial & Engineering Chemistry Process Design & Development* 24(2), 304-311. DOI: 10.1021/i200029a015

Vázquez, G., Antorrena, G., González, J., and Freire, S. (1997). "FTIR, ^{1}H and ^{13}C NMR characterization of acetosolv-solubilized pine and eucalyptus lignins," *Holzforschung - International Journal of the Biology, Chemistry, Physics and Technology of Wood* 51(2), 158-166. DOI: 10.1515/hfsg.1997.51.2.158

Xu, C., and Etcheverry, T. (2008). "Hydro-liquefaction of woody biomass in sub- and super-critical ethanol with iron-based catalysts," *Fuel* 87(3), 335-345. DOI: 10.1016/j.fuel.2007.05.013

Yamada, T., and Ono, H. (1999). "Rapid liquefaction of lignocellulosic waste by using ethylene carbonate," *Bioresource Technology* 70(1), 61-67. DOI: 10.1016/S0960-8524(99)00008-5

Yan, R., Yang, H., Chin, T., Liang, D. T., Chen, H., and Zheng, C. (2005). "Influence of temperature on the distribution of gaseous products from pyrolyzing palm oil wastes," *Combustion & Flame* 142(1–2), 24-32. DOI: 10.1016/j.combustflame.2005.02.005

Yao, Y., Yoshioka, M., and Shiraishi, N. (1995). "Rigid polyurethane foams from combined liquefaction mixtures of wood and starch," *Mokuzai Gakkaishi* 41(7), 659-668.

Yao, Y., Yoshioka, M., and Shiraishi, N. (1994). "Soluble properties of liquefied biomass prepared in organic solvents. I. The soluble behavior of liquefied biomass in various diluents," *Journal of the Japan Wood Research Society* 40(2), 176-184.

Yip, J., Chen, M., Szeto, Y. S., and Yan, S. (2009). "Comparative study of liquefaction process and liquefied products from bamboo using different organic solvents," *Bioresource Technology* 100(24), 6674-8. DOI: 10.1016/j.biortech.2009.07.045

Yoshida, C., Okabe, K., Yao, T., Shiraishi, N., and Oya, A. (2005). "Preparation of carbon fibers from biomass-based phenol-formaldehyde resin," *Journal of Materials Science* 40(2), 335-339. DOI: 10.1007/s10853-005-6087-1

Yu, F., Liu, Y., Pan, X., Lin, X., Liu, C., Chen, P., and Ruan, R. (2006a). "Liquefaction of corn stover and preparation of polyester from the liquefied polyol," *Applied Biochemistry & Biotechnology* 130(1-3), 574-585. DOI: 10.1385/ABAB:130:1:574

Yu, F., Liu, Y., Pan, X., Lin, X., Liu, C., Chen, P., and Ruan, R. (2006b). "Liquefaction of corn stover and preparation of polyester from the liquefied polyol," *Applied Biochemistry & Biotechnology* 129-132(1-3), 574. DOI: 10.1385/ABAB:130:1:574

Zhang, Q. H., and Zhao, G. J. (2014). "Research progress on mechanism of wood liquefaction reaction in phenol and polyhydric alcohols," *Chemistry & Industry of Forest Products* 22(4), 137-143. DOI: 10.3969/j.issn.0253-2417.2014.04.024

Article submitted: April 23, 2018; Peer review completed: July 14, 2018; Revised version received and accepted: July 19, 2018; Published: July 25, 2018.
DOI: 10.15376/biores.13.3.6818-6836